Bulletin of Engineering Geology and the Environment (2020) 79:3649–3666
https://doi.org/10.1007/s10064-020-01803-0

ORIGINAL PAPER

Development of a combined mining technique to protect the underground workspace above confined aquifer from water inrush disaster

Shengchao Yu[1,2,3] · Jingmin Xu[4] · Weibing Zhu[1,2] · Sihua Wang[2] · Wenbing Liu[2]

Received: 26 August 2019 / Accepted: 8 April 2020 / Published online: 24 April 2020

Abstract

One task facing by the geotechnical engineers is to protect the workspace in an underground construction/excavation site from various forms of geological disasters, such as the water inrush, rock burst, and collapse of the surrounding rock/soil. In this paper, a combined controlling measure was proposed based on underground mining and water environment: the method of strip mining has been initially proposed as an effective measure against underground workspace floor failure when mining above confined aquifer in the Bucun coal mine, China, and however, its ability to avoid floor water inrush has yet to be demonstrated; in the next step, field trials using caving zone backfill technology to prevent underground workspace floor failure and excavate retained strip coal pillars were implemented based on the theoretical calculation and numerical simulation results. Engineering practice showed that the failure depth of the underlying strata of the workspace had no growth without the possibility of water inrush, and the safety of the underground space was achieved. Thus, this study represents a successful attempt to develop the combined strip mining and caving zone backfilling technique to ensure the safety of the underground workspace and control surface subsidence when excavating the retained strip coal pillars above confined aquifer. The proposed combined technique can also be used in other underground excavation activities with similar problems.

Keywords Underground workspace safety · Floor water inrush · Strata failure depth · Combined technique · Strip mining · Caving zone backfilling

Notationa list

Bul (Pa)	Bulk modulus of strata
CP (m)	Failure depth of seam floor after strip mining
Coh (Pa)	Cohesion of strata
d (m)	Depth of strata
D1 (m)	Depth of each drilling borehole
D2 (m)	Distance between coal seam and each aquifer
Den (kg/m^3)	Density of strata
F (–)	Safety factor of coal pillar
Fric (deg)	Internal friction angle of strata
Gro (–)	Layer no. group of strata
h (m)	Mining height of working face
H (m)	Cover depth of coal seam
M (m)	Thickness of aquiclude
n (–)	A constant that depends on the ratio of width to height of the retained coal pillar
P (MPa)	Water pressure sustained by coal seam floor
*P*p (MPa)	Load on strip coal pillar

✉ Jingmin Xu
jingmin.xu@nottingham.ac.uk

[1] State Key Laboratory of Coal Resources and Safe Mining, China University of Mining and Technology, Xuzhou 221116, China

[2] Key Laboratory of Deep Coal Resource Mining, Ministry of Education of China, School of Mines, China University of Mining and Technology, Xuzhou 221116, China

[3] Department of Earth Sciences, The University of Hong Kong, Hong Kong 999077, China

[4] Department of Civil Engineering, Faculty of Engineering, University of Nottingham, University Park, Nottingham NG7 2RD, UK

Shea (Pa)	Shear modulus of strata
t (m)	Thickness of strata in geologic column
T (m)	Thickness of aquifer
Ts (–)	Water inrush coefficient
Ten (Pa)	Tension of strata
Thic (m)	Thickness of strata in numerical model
W1 (m^3/h)	Water yield of aquifer
W2 (m)	Water level of aquifer
We (m)	Width of excavated coal pillar
Wp (m)	Width of retained coal pillar
γ (N/m^3)	Average bulk density of overlying strata
σm (MPa)	In situ strength of coal pillar
σp (MPa)	Bulk unit weight of strip coal pillar

Introduction

The surroundings of underground coal mining are complex and the lower and upper strata close to the coal seams might have rich water, so there is a potential risk of floor water inrush when mining coal resources above confined aquifer especially when there is an obvious failure depth of seam floor (Guo et al. 2018; Ma et al. 2013, 2015; Malkowski et al. 2014, 2017; Wu and Wang 2006). For instance, a maximum water inrush flow rate of 34.22 m^3/s occurred in the Fangezhuang coal mine of Kailuan, China, causing an economic loss of up to 500 million yuan (Meng et al. 2012; Meng et al. 2018). In Zhaogezhuang coal mine as well, groundwater burst along the fault zone around tram rail and ventilating way, indicating that the fault zone played an important role in inducing the groundwater bursting (Wu et al. 2004). Statistically, 285 coal mines suffer from mine water hazards, taking up 47.5% of the country's over 600 state-owned key coal mines in China (Wu et al. 2004). Over 25 billion tons of coal resources are at potential risk of floor water inrush (Xu and Wang 1991; Zhang and Shen 2004).

The threat of floor water inrush affects the production and safety of coal mines, which is a common issue that mining engineers try to address (Zhang et al. 2017a, b). How to predict whether the floor water inrush would happen or not and how to prevent it have gradually caused more studies. Since the 1940s, the study on mechanism of water inrush has attracted attention of international researchers, and the problem of water inrush has gained more attentions in China since the 1960s (Li and Zhang 1995; Qian et al. 1995). The theoretically derived calculation formula of floor water inrush coefficient, in overall consideration of the aquiclude thickness, hydraulic pressure of aquifer, and failure depth of seam floor, is usually applied to calculate and statistically analyze the possibility of water inrush (Liu 2009; Sawsc 2009). Based on this, Li et al. (2018) established an improved vulnerability assessment model, taking high water pressure and lower water yield into consideration to further be successfully applied in the practice of Huaibei mining area, China. In addition, more assessment methods, such as vulnerability index method (Wu and Zhou 2008), analytic hierarchy process (Wu et al. 2013), geographic information system (GIS)-based analytic hierarchy process (Wu et al. 2011), GIS-based Bayesian network (Dong et al. 2012), micro-level aquifer mapping and management (Chatterjee et al. 2018), and maximizing deviation in a GIS environment (Yang et al. 2018a), are used worldwide to predict the possibility of floor water inrush.

Generally, the prevention of floor water inrush can be processed from two stages. Prior to the exploitation of coal seams, the design of reasonable mining scheme can be conducted based on the abovementioned theories. For example, when there is a potential of fracture, breakage, and further water inrush for seam floor, the method of strip mining as an effective means, since causing small water flowing fracture zone, is usually applied to exploit coal resources under buildings and above or under confined aquifer to achieve water protection mining (Gao and Ge 2016; Mark and Agioutantis 2019; Yin et al. 2009; Zhang et al. 2011; Zingano and Weiss 2019). But the anticipated prediction and designed mining scheme cannot 100% sure to avoid the occurrence of water inrush accident and a mass of coal pillars are retained as well, especially when employing the method of strip mining. Then how to treat the loss of coal resource and repair the generated seam floor failure becomes the next question. Accordingly, during or after coal mining, there are some primary remedial engineering measures used to prevent water inrush from confined aquifers underlying coal seams (Cai et al. 2019; Junthong et al. 2019; Meng et al. 2018; Niedbalski et al. 2018; Palarski et al. 2011, 2014; Strozik 2017). One measure is draining the aquifer to lower the pressure on the aquiclude, but the aquifer is usually so thick that the aquifer is usually overdrained over long period without knowing how much water should be drained, which leads to many environmental problems (Meng et al. 2018). The other measure is grouting to block fractures in the aquifer, which also strengthens the water-resisting ability of the aquiclude, while the method of excavating strip coal pillars using caving zone backfill technology is evolving based on this aforesaid thought (Meng et al. 2018; Zhu et al. 2018b). As for the caving zone backfill technology, the slurry is grouted into goaf rather than aquifer or aquiclude to limit the damage of seam floor from its upward side. The formed backfilling body cannot only support the weight of overlying strata to further control surface subsidence, but also provide a safe zone for exploiting the coal pillars retained in earlier stage due to the consideration of security issue. These related studies have been represented in authors' previous work (Zhu et al. 2018b); then, whether the caving zone backfill technology can prevent the further failure of seam floor and repair the generated failure to prevent water inrush is still unknown.

In this study, the coal seam No. 9-1, whose coal quality is so pretty that should be completely mined, is located above a confined aquifer with a lot of buildings constructed on the ground, so the rule of safe mining is required in view of not only protecting surface buildings but also preventing from floor water inrush. Previously, excavating strip coal pillars using caving zone backfill technology has been implemented in Bucun coal mine to analyze the issues about retained strip coal pillars and surface subsidence (Zhu et al. 2018b), but no research works have been able to study sufficient control over seam floor's failure and effective prevention about floor water inrush. This study tested these unsolved issues by proposing a controlling measure combined by strip mining method and caving zone backfill technology, as shown in Fig. 1, providing

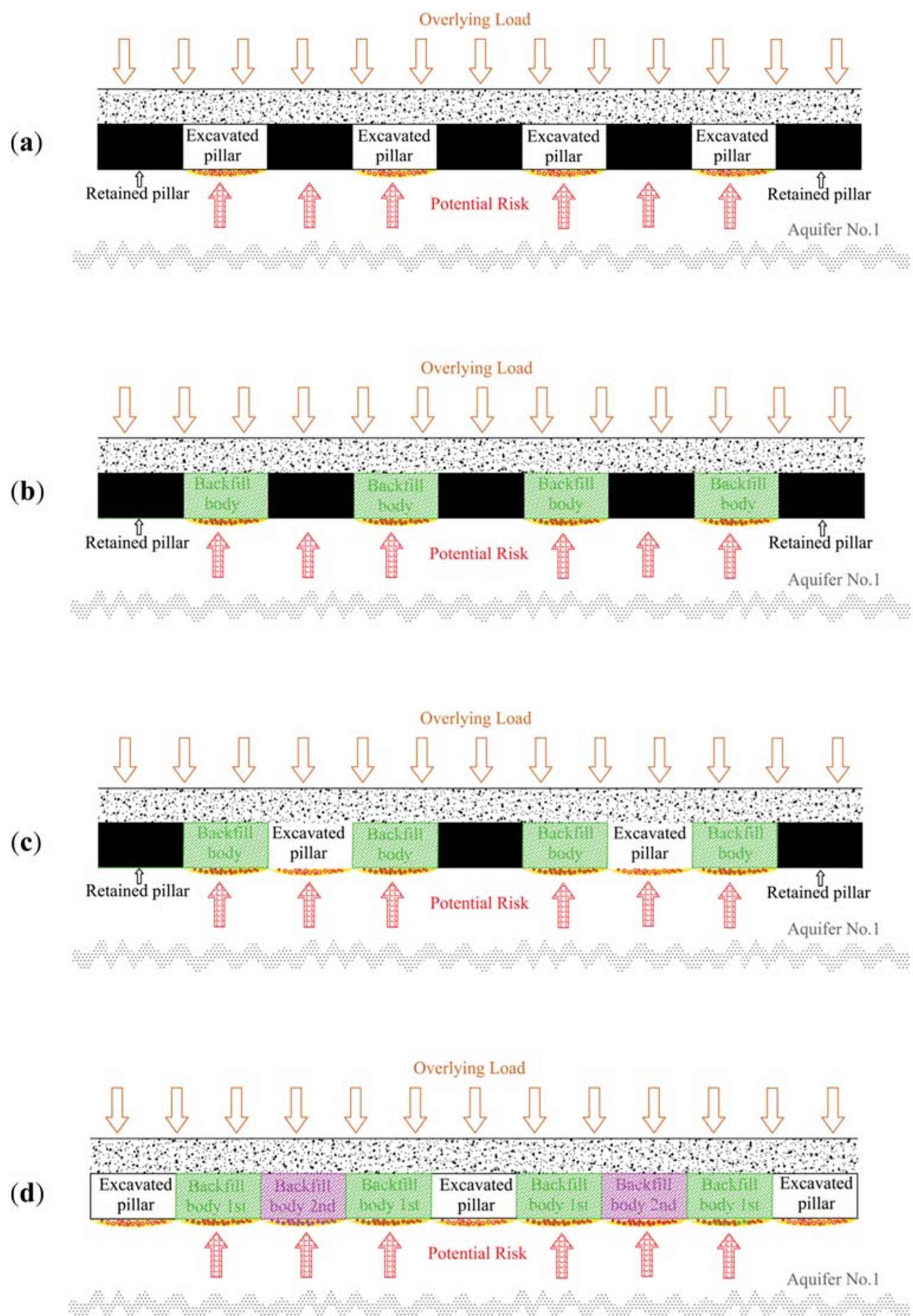

Fig. 1 Schematic illustration combined technique. **a** Strip mining. **b** Backfilled original caving zones. **c** Retained pillar excavation. **d** Backfilled new caving zones

guidance and acting as reference for similar trials investigating the seam floor's failure and preventing floor water inrush when coal mining above confined aquifer.

Materials and methods

Theoretical background

Based on the engineering practice adopting strip mining method (Fig. 1a), the need for excavating retained strip coal pillars, controlling surface subsidence, and preventing floor water inrush had arose further consideration and then the caving zone backfill technology was proposed, since the generated floor failure zone can be backfilled (Fig. 1b) so that the retained coal pillars could be excavated (Fig. 1c) as well as prevent floor failure (Fig. 1d). That is the controlling measure combined by strip mining and caving zone backfill technology to prevent the potential risk of water inrush from seam floor.

In view of the mining area shown in Fig. 1a, the processes of this combined controlling measure are presented as follows. First, the coal seam is exploited using strip mining method, with certain coal pillars, which are supposed to control surface subsidence, retained in the working face (Fig. 1a); then, the caving zone, meaning the white block in Fig. 1a, is grouting injected with high-water content material until the gap in the gangue is fully filled (Fig. 1b), creating a combined backfill body of caved gangue and high-water content material, as shown in the green block in Fig. 1b; after the combined backfill body solidifies and achieves a certain strength, original strip mining face can be set up to excavate the retained strip pillar (Fig. 1c); Fig. 1d shows the final state of this controlling measure, which means the original caving zones in Fig. 1a must be backfilled, and the new caving zone after high-water content material backfilled once are optional to be backfilled.

Site description

Location of the study site

The Bucun coal mine is located in Zhangqiu, Shandong Province, China. It is operated by the Zibo Mining Group Co., Ltd. and commenced operation in 1958. The occurrence status of coal seam No. 3 is comparatively regular so it was once the main mineable seam in this mining area. However, although the occurrence status of coal seam No. 9-1 is the same regular, the potential of floor water inrush for this coal seam is particularly serious since its floor is close to confined aquifers, so the unexploited coal seam No. 9-1 is currently regarded as the main research subject. Some buildings are located on the ground right above the studied mining district, such as Shanhouzai village, town government, township hospital, post and telecommunications office, geracomium, residential buildings, and the national highway, as shown in Fig. 2. On the basis of constructing times of these buildings, only a few are simultaneously affected when mining coal seams Nos. 3 and 9-1, and the overwhelming majority are only affected by the late production of coal seam No. 9-1.

Geology and mining conditions

The burial depth of this study mining area termed as 911, as the initial district, is 390 m and coal seam No. 9-1 is mainly deployed. The length along the strike is 260–1430 m and the width along the dip is 400–780 m. The average thickness of the coal seam is 1.3 m and the average dip angle is 9.5°, with its cover depth ranging from 345 to 480 m. The texture of coal seam is simply with stable occurrence. Table 1 shows the geologic borehole column of mining area 911.

According to data of nine underground boreholes in working face 9111 and nearby, as shown in Table 2, it can be analyzed that aquifer No. 1 is developed in mining area 911 with the average distance from coal seam No. 9–1 at 58.25 m and its depth is 3.49–27.84 m with an average of 13.88 m. The water yield in a single hole is 2.8–246 m^3/h and the water level is ranging from − 231.4–46.7 m. In view of hydrogeological exploration, geophysical prospecting, and boreholes data, the water yield property of aquifer No. 1 is great as well as the water conservancy contact, and the water in this aquifer is supplied by vertical cross flow from underlying aquifer No. 2 so the water quality and water level of these two aquifers are similar. Aquifer No. 2 is located in the basement of coal measure strata which is the main aquifer in this mining area. From the data of borehole 911-ox1 in aquifer No. 2, it can be indicated that this aquifer is 84.29 m away from coal seam No. 9-1. From the abovementioned data, the geological profile map can be concluded as shown in Fig. 3. The detailed hydrogeological conditions will be presented in the following subsection.

The coal seam No. 3, right above this mining area 911, was exploited from 1997 to 2001 by using the method of strip mining along the dip. The actual average mining height was 1.2 m, and the width of the excavated strip was 40–55 m and that of the retained strip was 20–40 m. It is statistically analyzed that the recovery ratio was only 44%. Since there is an average distance of 124 m between coal seam Nos. 3 and 9-1, the method of strip mining was initially proposed for the exploitation of coal resources in mining area 911 from 2005 to 2009, in order to control surface subsidence and prevent floor water inrush from aquifer Nos. 1 and 2, which is also the first process of the studied controlling measure.

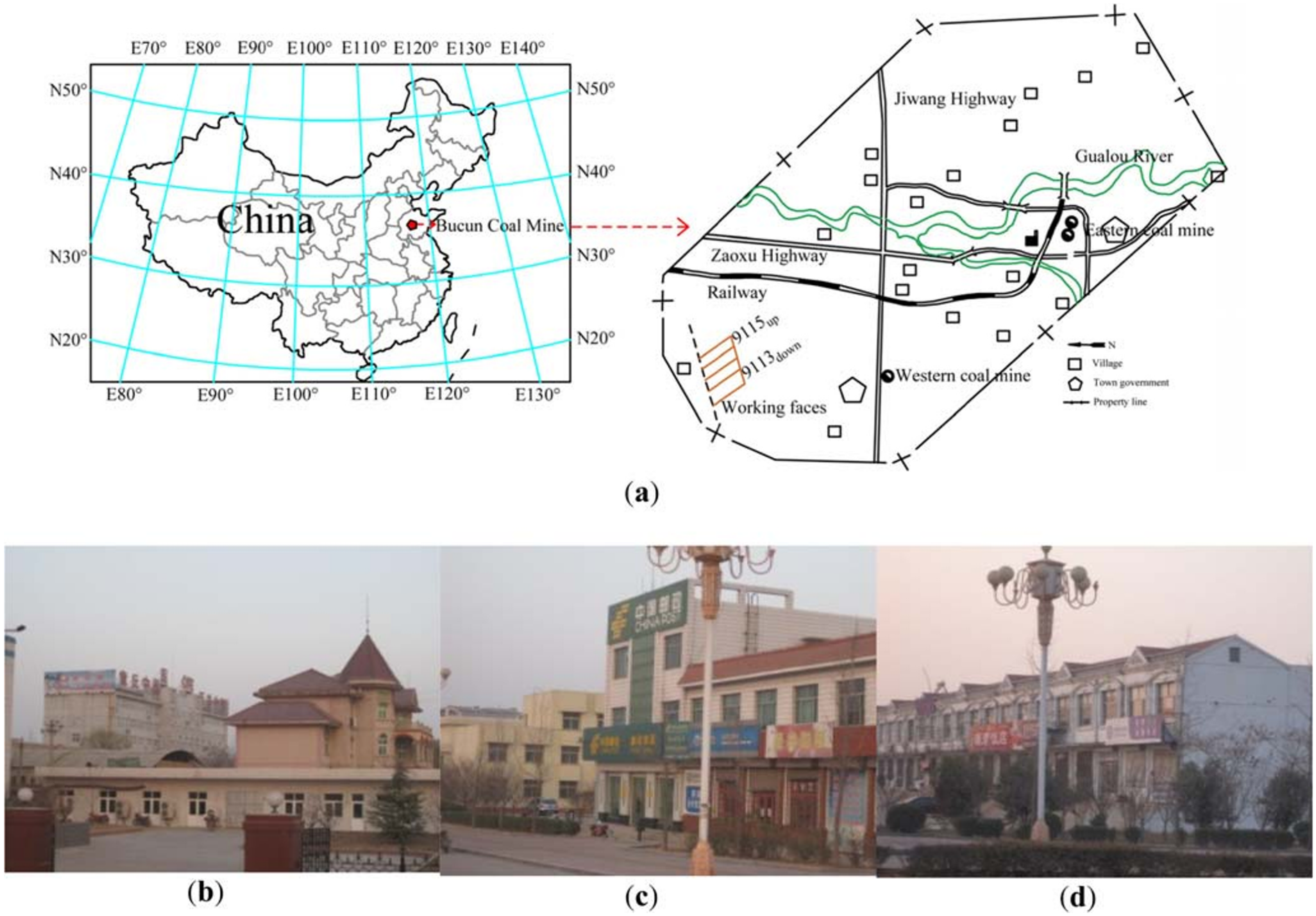

Fig. 2 Map of the Bucun coal mine. **a** Location and layout of the Bucun coal mine. **b** Township hospital. **c** Post office. **d** Residential buildings

Hydrogeological conditions

After the excavation of coal seam No. 9-2 which had a serious potential of floor water inrush from confined aquifer with high pressure in Bucun coal mine during the 1970s, there were gradually some early insights into water inrush problem of seam floor in this coal mine. What should be carefully noticed is that the thickness of aquifer and aquiclude is the basic factor restricting water inrush. According to previous cases of water inrush, when the water inrush coefficient of aquifer No. 1 was up to 0.08 MPa/m in the excavation of coal seam No. 10-1 under normal geological conditions, the water inrush accident occurred, while it did not occur when excavating coal seam No. 9-2 in the same region. This is mainly because the thickness of aquiclude in the latter is increased by about 17 m compared with that of the former. Therefore, this is also the main evidence that the failure depth without growth can be used to determine no floor water inrush in this study, which can be further applied to prove that no water inrush is primarily due to the newly proposed method. At the same time, other hydrogeological conditions of this coal mine will be introduced below in order to better illustrate this problem.

As is known to all, the development of geological structures is a significant factor affecting water inrush from seam floor (Wu et al. 2004; Zhang 2005; Zhang and Shen 2004). Faults and fracture zones destroy the integrity of aquiclude and impact its water isolated capacity, and hence the small fault dense zone with small drop is also an important element inducing water inrush. For example, there were two strike faults and two inclined faults in the working face 9091 with the burial depth at 290.3 m; when this working face was advanced to 85 m, the floor water inrush accident occurred at the intersection of small faults. While as for working face 9090 with a burial depth at 354.0 m, there was no water inrush accident occurred due to fault nondevelopment here. Mining area 911 mentioned in this study, close to the working face 9090, has a cover depth at 390 m and there is no major fault in this mining area. Therefore, it is reasonable to exclude the factor of geological structures in the analysis of floor water inrush.

Based on the disciplines of floor water inrush which occurred when excavating coal seam Nos. 9 and 10, the main factors affecting water inrush include not only the hydraulic head pressure, the thickness of aquiclude, and the fault fracture zone, but also the mine pressures, such as first weighting

Table 1 Geologic column section of the mining area 911

No.	*t* (m)	*d* (m)	Lithology	No.	*t* (m)	*d* (m)	Lithology
1	29.50	29.50	Topsoil	35	10.20	257.60	Medium sandstone
2	0.31	29.81	Chaos	36	11.40	269.00	Clay shale
3	6.89	36.70	Sandshale	37	6.60	275.60	Packsand
4	9.03	45.73	Medium sandstone	38	6.90	282.50	Sandshale
5	11.47	57.20	Sandshale	39	12.20	294.70	Packsand
6	5.80	63.00	Medium sandstone	40	15.00	309.70	Sandshale
7	2.78	65.78	Sandstone	41	11.80	321.50	Medium sandstone
8	22.81	88.59	Medium sandstone	42	0.20	321.70	Soft rock
9	1.65	90.24	Packsand	43	3.24	324.94	Sandshale
10	2.55	92.79	Medium sandstone	44	0.17	325.11	Soft rock
11	2.74	95.53	Sandshale	45	9.29	334.40	Sandshale
12	2.00	97.53	Medium sandstone	46	2.30	336.70	Packsand
13	9.57	107.10	Packsand	47	1.21	337.91	Sandshale
14	4.44	111.54	Varied shale	48	0.20	338.11	Soft rock
15	3.00	114.54	Packsand	49	0.89	339.00	Clay shale
16	5.30	119.84	Varied shale	50	7.00	346.00	Sandshale
17	2.00	121.84	Packsand	51	6.70	352.70	Sandshale
18	17.84	139.68	Varied shale	52	0.27	352.97	Cokeite
19	2.82	142.50	Packsand	53	3.63	356.60	Magmatite
20	36.16	178.66	Varied shale	54	3.20	359.80	Sandshale
21	1.05	179.71	Packsand	55	6.60	366.40	Mudstone
22	5.66	185.37	Varied shale	56	5.20	371.60	Packsand
23	4.31	189.68	Sandshale	57	13.28	384.88	Sandshale
24	4.62	194.30	Packsand	58	1.35	386.23	Seam 9-1
25	2.70	197.00	Fault zone	59	2.19	388.42	Packsand
26	4.34	201.34	None	60	4.30	392.72	Sandshale
27	5.66	207.00	Packsand	61	3.80	396.52	Packsand
28	9.20	216.20	Varied shale	62	7.11	403.63	Sandshale
29	4.80	221.00	Sandshale	63	1.45	405.08	Seam 10-1
30	8.00	229.00	Packsand	64	4.64	409.72	Clay shale
31	6.00	235.00	Sandstone	65	1.50	411.22	Medium sandstone
32	2.20	237.20	Sandshale	66	2.00	413.22	Mudstone
33	4.80	242.00	Sandstone	67	4.50	417.72	Medium sandstone
34	5.40	247.40	Sandshale	68	1.29	419.01	Sandshale

Table 2 Situations of aquifers detected by drilling boreholes

Borehole no.	D1 (m)	D2 (m)		Aquifer no. 1			Aquifer no. 2		
		No. 1	No. 2	*T* (m)	W1 (m^3/h)	W2 (m)	*T* (m)	W1 (m^3/h)	W2 (m)
1	− 352.8	65.01	–	13.39	240	34.8	–	–	–
2	− 345.6	61.46	–	10.44	120	42	–	–	–
3	− 362.2	58.12	–	4.53	90	35.6	–	–	–
4	− 381.7	58.22	–	3.49	246	46.7	–	–	–
S1	− 371.1	47.34	–	12.13	60	− 24.3	–	–	–
S2	− 350.5	55.4	–	12.53	35	45.18	–	–	–
Lxg12	− 381.4	62.56	–	11.93	12	− 197.8	–	–	–
911-ox1	− 384.4	65.23	84.29	8.88	2.8	− 231.4	31.22	–	–
S3	98.9	55.22	–	27.84	–	–	–	–	–

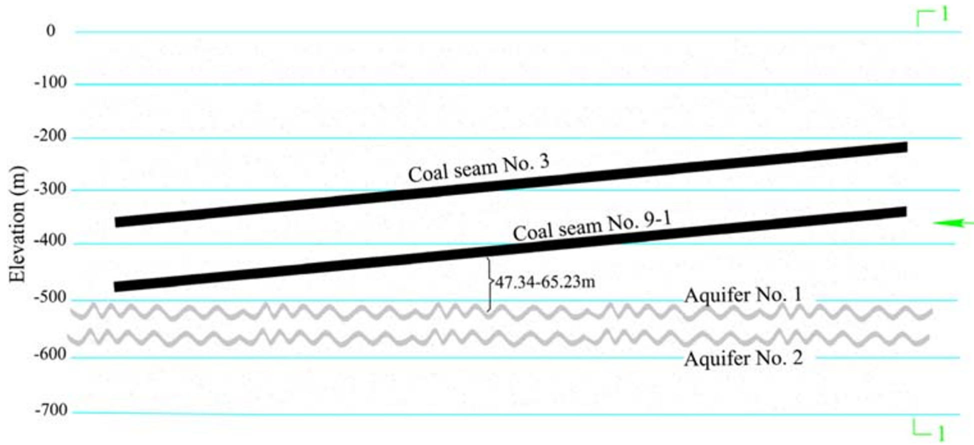

Fig. 3 Geological profile map of the Bucun coal mine

and periodic weighting. According to the observation data of mine pressure in the west wing of Bucun coal mine, the first roof weighting interval is 32 m, which is also the main reason of water inrush in the later working face 9110 (see the "Floor water inrush accident" section). However, when there is a potential of floor water inrush and the mining induced underground pressure is excluded from the caused reasons, which means that the potential threat point of water inrush is not within the range of first weighting and periodic weighting, there are reasons to believe that the thickness of aquifer and aquiclude could be the basic factor restricting water inrush.

Proposed strip mining method

The great advantage of strip mining method is the low cost for mining per ton coal under the premise of unchanged mining technique. It has the simple technology with the uncomplicated production management, and surface subsidence can be dramatically reduced with the lowered failure depth of seam floor (Gao and Ge 2016; Zhang et al. 2011; Yin et al. 2009). Existing field practice and theoretical study show that strip mining method is always an effective means of safely excavating the coal resource under buildings and above confined aquifer, which is also the primary cause for initially proposing this step to exploit coal resources in consideration of the geological conditions of Bucun coal mine.

Floor water inrush accident

Working face 9110, as the first mining face, was arranged in mining area 911. It was being mined on July 15, 2004 using the strip mining method with the width of the excavated strip at 40 m. When this working face was advanced about 33 m at 13 o'clock on July 31, the roof caved after first weighting, leading to floor water inrush at the back of working face. The initial water yield was 150 m^3/h and the maximum, as the steady yield, was 334.8 m^3/h. Water inrush occurred as soon as the roof caving and first weighting in working face, which indicated that mining-induced underground pressure is the key factor for water inrush.

After this accident, the grouting plugging was timely implemented, and this working face was put back on production on August 2005. After the success of water plugging, it is studied that the stopping technology needed to be altered to strip mining along the dip, with preliminary adjustments for the widths of excavated and retained strips as well as the recovery method, to prevent floor water inrush and protect surface buildings with effect. Therefore, the limitation of strip mining method in this study site still be worthy of discussion, i.e., whether this strip mining scheme can meet the needs of safe mining above confined aquifer needs to be further analyzed.

In order to facilitate the following analysis of strip mining parameters, the mining situations of adjacent working faces were listed in Table 3, and the involved working faces placement can be seen as shown in Fig. 4. After the accident of floor water inrush in working face 9110, the stopping technology here altered to strip mining along the dip with the width of excavated strip at 15 m and that of retained strip at 20 m. By referring to the safe stopping experience in working face 9110, the method of strip mining along the dip was adopted in working faces 9112, 9114, and 9116 with the same widths of excavated and retained strips as working face 9110 but besides the working face 9118 adopting the width of excavated strip at 20 m since it was located in the shallowest level.

Parameter determination

Engineering practice showed that all the abovementioned working faces achieved safe and high-efficiency mining. Therefore, in order to prevent floor water inrush and protect surface buildings with effect, it is planned that working faces at the west wing of mining area 911 initially adopted the method of strip mining along the dip with the widths of excavated strip at 15 m and retained strip at 20 m but besides some

Table 3 Mining situations of working faces at the east wing of mining area 911

Mining sequence	Working face no.	Width of excavated strip (m)	Width of retained strip (m)	Remarks
1	9110	15	20	Deepest
2	9112	15	20	/
3	9114	15	20	/
4	9116	15	20	/
5	9118	20	20	Shallowest

shallow levels with the width of excavated strip at 20 m, for instance working face 9115.

Generally, the stability of strip coal pillar needs to be analyzed after determining its parameters. To verify whether the proposed parameters of strip mining can be used in current mining conditions, the strength of strip coal pillar was initially checked by introducing the ultimate strength theory here (Bieniawski 1981; Zhu et al. 2017, 2018a). In order to guarantee the long-term stability of coal pillar, the safety factor should be normally from 1.2 to 2.0.

$$F = \frac{\sigma \mathrm{p}}{P\mathrm{p}} = 1.2\sim 2.0 \tag{1}$$

where F is the safety factor of coal pillar, 1;σp is the strength of strip coal pillar, MPa; and Pp is the load on strip coal pillar, MPa. The calculation formula for the load on strip pillar can be expressed as:

$$P\mathrm{p} = \gamma H\left(1 + \frac{W\mathrm{e}}{W\mathrm{p}}\right) \tag{2}$$

where γ is the bulk unit weight of overlying strata, N/m^3; H is the cover depth of coal seam, m; We is the width of excavated coal pillar, m; and Wp is the width of retained coal pillar, m. The calculation formula for the strength of strip coal pillar is given as:

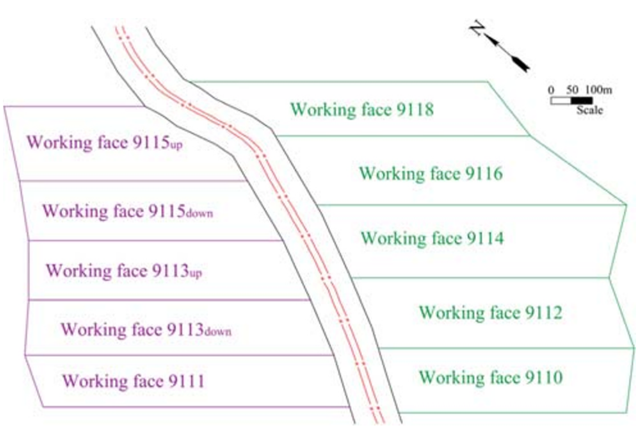

Fig. 4 Working face locations in mining area 911

$$\sigma \mathrm{p} = \sigma \mathrm{m}\left(0.64 + 0.36\frac{W\mathrm{p}}{h}\right)^n \tag{3}$$

where σm is the in situ strength of the coal pillar, MPa; h is the mining height of working face, m; and n is a constant that depends on the ratio of width to height of the retained coal pillar: when, $W\mathrm{p}/h > 5$, $n = 1.4$, and when $W\mathrm{p}/h < 5$, $n = 1$.

The maximum burial depth at which the backfilling body was located in mining area 911 was 480 m, and the mining height was 1.3 m. The uniaxial compressive strength (UCS) of 9-1 coal samples was 8.67 MPa and the calculated in situ strength of the coal mass was 2.04 MPa (Zhu et al. 2018b). The strip mining working face was mined with the widths of excavated strips at 15 m and retained strips at 20 m. Substituting these parameters into the abovementioned formulas is used to calculate the safety factor, 1.4, which was larger than its setting value. It can be seen that the proposed strip mining method in mining area 911 can ensure the long-term stability of coal pillar.

Floor failure depth prediction

In order to check whether the proposed strip mining scheme can avoid the floor water inrush accident or not, FLAC software, as the finite difference simulation software, was employed to simulate the mining-induced failure depth of No. 9-1 seam floor. Two dimensions were considered while ignoring the factor of coal seam strike. It is reasonable that the mining process is not considered, since the working face is narrow and then the numerical model can be regarded as a plane-strain model along the mining direction. In view of this 9.5° average dip angle of seam belonging to flat seam (Bondarenko et al. 2010), which can be regarded as simplified horizontal layer in the model, the influence of the dip angle of coal seam was ignored but the possible effect on the predicted failure result will be discussed later. In fact, the detecting boreholes are not sufficiently enough to perfectly reveal the conditions of aquifers, and as a consequence, the precise distance between coal seam and aquifers and the specific hydraulic pressures of aquifers are unknown. However, as for the related setting in numerical model, it is well-known that as a type of stress applied on the bottom of the seam floor, water

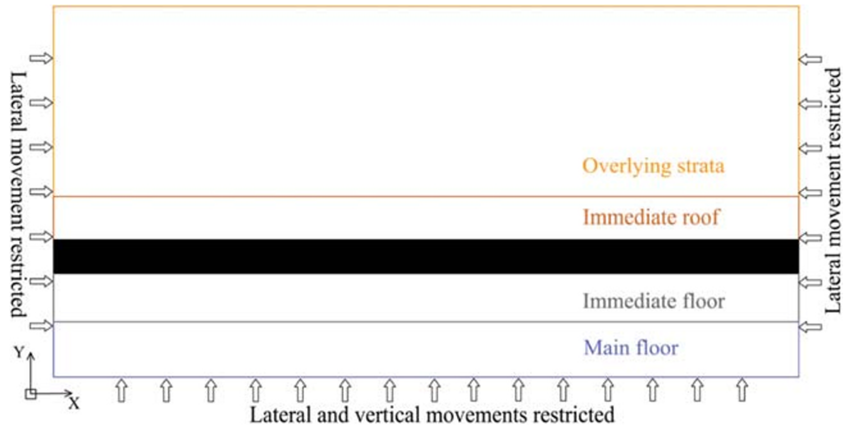

Fig. 5 Schematic diagram of numerical model for strip mining

pressure makes the floor strata much easier to expand into the exposed space of the mined area, causing a bigger seam floor failure depth (Zhang 2005). Since rock permeability is known to strongly correlate with the rock characteristics (e.g., fracture properties and lithology), in order to analyze the influence of the hydraulic pressure on the deformation and failure of the coal seam floor (Huang et al. 2016; Huang et al. 2019; Ma et al. 2019; Yang et al. 2011), the effect of water pressure on rock fracture was considered in the model. Importantly, it should be mentioned that this simplified numerical simulation was only a preliminary prediction on the coal seam failure depth by considering the effects of extracting retained coal pillars and implementing backfilling activities prior to engineering practice. Overall, this is an engineering experience orientated study, and the measured engineering data mentioned later can provide strong evidence that the proposed method is effective.

Based on the geological data of mining area 911 in Bucun coal mine listed in the "Geology and mining conditions" subsection, the corresponding 2D numerical model was set up to verify the reasonability of setting mining parameters, as shown in Fig. 5, with Table 4 listing the strata characteristics and mechanical parameters. The designed model with 400 m length and 200 m height includes the depth of seam floor at 50 m and the distance from floor to the top of model at 150 m. The upper model means the overlying strata of coal seam and the lower model means the floor beneath coal seam. The model domain was divided into 80 lines and 80 column quadrangles, so the mesh grid contains 6561 nodes and 6400 quadrangle elements in total. In order to better manifest the failure status of seam floor, uniformly-spaced mesh generation was not employed vertically while partial refinement was adopted. The mesh size varies from 0.52–3.60 m vertically with certain horizontal length at 5 m, and the related layer information can be seen in Table 4.

As described before, the two-dimensional finite element model was adopted in this simulation. The left and right boundaries and the bottom boundary are the displacement boundary conditions, and the top boundary is the stress boundary conditions. The boundary condition of the left side is the same as that of the right side with the lateral movement restricted, and that of the bottom side is both lateral and vertical movement restricted. Mohr-Coulomb yielding criteria are used in this model calculation. It is because of this that the scope of plastic failure zone can represent the failure degree of floor under different mining schemes. In addition, the main purpose of this model is to simulate failure depth of seam floor and since the controlling measure combined by strip mining and caving zone backfill technology is applied, the movement and deformation of rock strata have been effectively controlled, so it is feasible that the characteristics of overlying strata are simplified, which means the rest of rock strata are simulated by loading mode. In other words, there is a uniformly distributed load of 6.5 MPa on the top of the model.

Table 4 Mechanics parameters of each stratum in the numerical simulation

Stratum lithology	Thic (m)	Bul (Pa)	Shea (Pa)	Den (kg/m^3)	Fric (deg)	Coh (Pa)	Tens (Pa)	Gro (−)
Rock strata	144	8e9	8e9	2400	25	6.0e6	2.0e6	41–80
Immediate roof	4.7	6e9	6e9	2200	22	6.0e6	2.0e6	32–40
Coal seam	1.3	5e9	4e9	1350	22	1.5e6	8.0e5	31
Immediate floor	20	1e9	1e9	2500	20	3.3e6	1.5e6	11–30
Main floor	30	1e9	1e9	2500	20	3.3e6	1.5e6	1–10

There were mainly three steps for the numerical simulation process. The first step was balance computation of primary rock stress, then excavating coal seam No. 9-1 using strip mining with the widths of excavated strip at 15 m and retained strip at 20 m. The last step, i.e., the final process of proposed controlling measure for floor water inrush, was stated in the "Influence on floor failure depth" subsection. The specific excavation scheme of this numerical model during strip mining period can be seen as follows: the layer No. 31 in the model as the coal seam group was excavated from the block No. 21, keeping four blocks for every three blocks mined until reaching the block No. 58. Figure 6a shows the stress contour of surrounding rock after strip mining, Fig. 6b shows the scope of plastic failure zone of floor after strip mining, and Fig. 6c shows the distributions of the different failure values in each strip pillar respectively. It can be manifested that failure scope of surrounding rock was small and there was a plastic failure zone of 9 m in floor meaning the failure depth of seam floor.

Results and discussion

Field investigation during strip mining and comparison with numerical results

Field investigation

From 2005 to 2009, the method of strip mining along the dip was adopted in mining area 911, and approximately 490,000 t of coal was excavated while around 941,700 t of coal was retained in the pillars and the recovery ratio was only 34.2%. During this period, for the sake of monitoring the failure depth

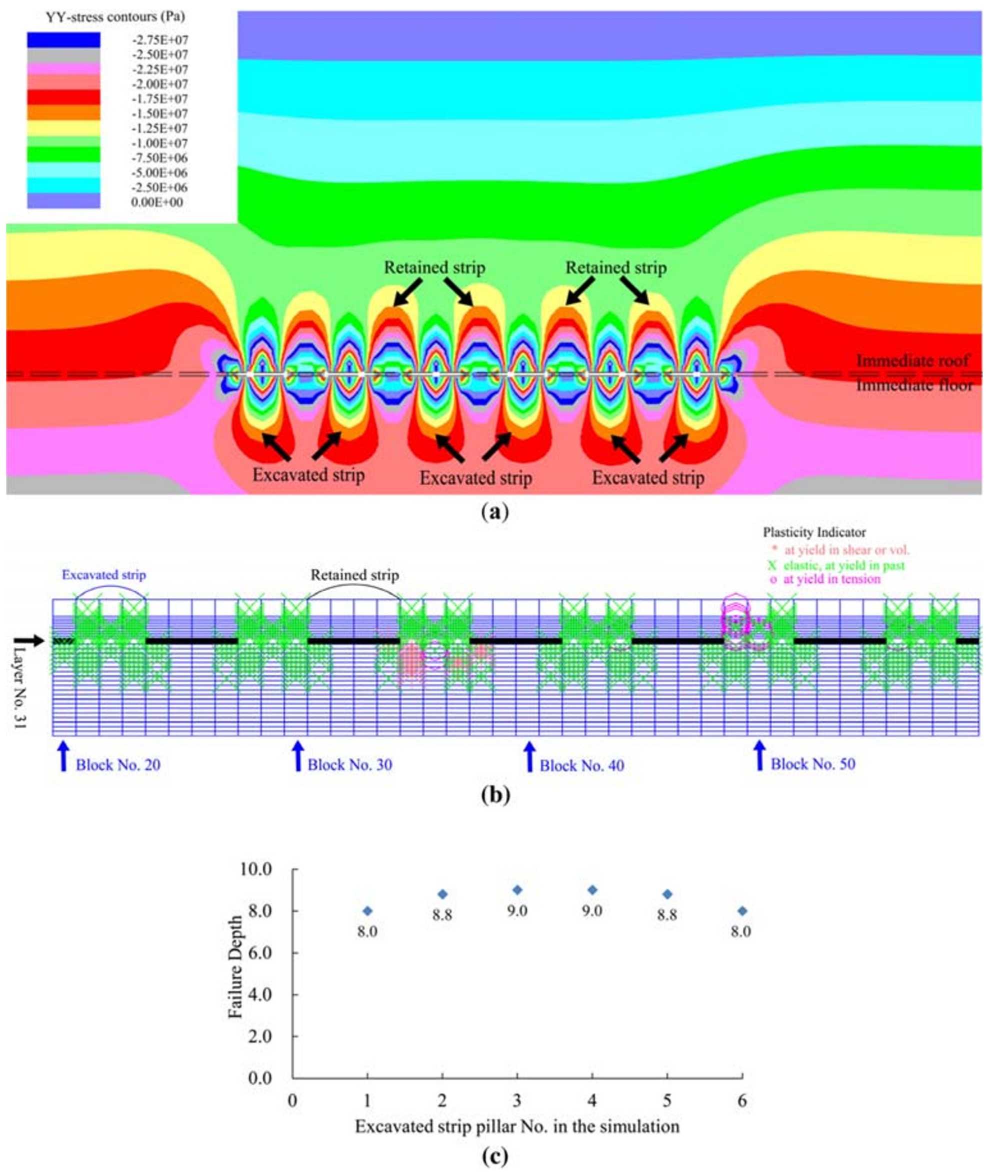

Fig. 6 Numerical results after strip mining. **a** Vertical stress distribution contour. **b** Scope of plastic failure zone of floor. **c** Distribution of the different floor failure values in each strip pillar

Fig. 7 Layout of monitoring system for seam floor's failure

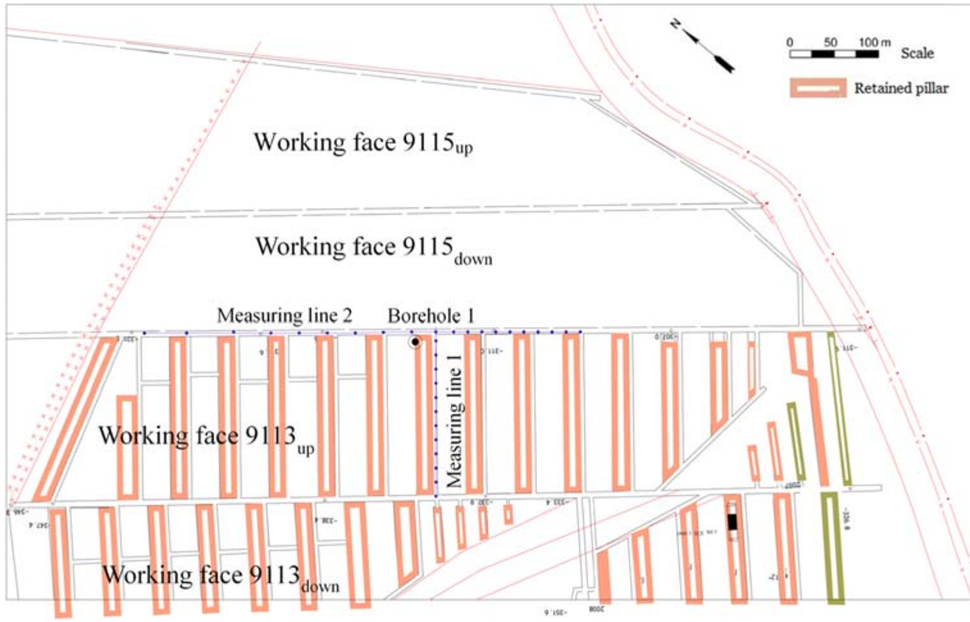

of floor in mining area 911 during strip mining, Anhui Huizhou Institute of Subterranean Calamity was invited to do the field measurement by means of parallel electrical survey system, angular displacement, and micro-seismic monitoring.

Working face 9113 is located in the west wing of mining area 911, adopting the method of strip mining along the dip with the widths of excavated strip at 15 m and retained strip at 20 m. The monitoring system for the seam floor's failure was arranged from lateral, longitudinal, and vertical directions to guarantee a holistic and all-round monitoring for floor. Figure 7 shows the layout of these monitoring systems. The lateral measuring line, measuring line 1, was set in the open-off cur of working face and the longitudinal measuring line as measuring line 2 was set in the upper exit, and the vertical measuring line was set in the borehole 1 which was specially constructed. The probes of parallel electrical survey system, angular displacement sensors, and sound emission microphones were installed in each measuring line.

Figure 8 shows the profile map of the apparent resistivity in measuring line 1. The result of this electrical survey on the figure was selected based on profile map data of the apparent resistivity in mine roadway, i.e., the longitudinal measuring line as measuring line 2 of 141 m was set with the middle at the ninth excavated coal pillars in order to make the effective detection range up to the width of one excavated pillar and two retained pillars. During the observation in mining-induced period, it was found that the electrical resistivity in the below of the goaf was higher than that in the below of coal pillars with arc low resistivity zone formed there. That means

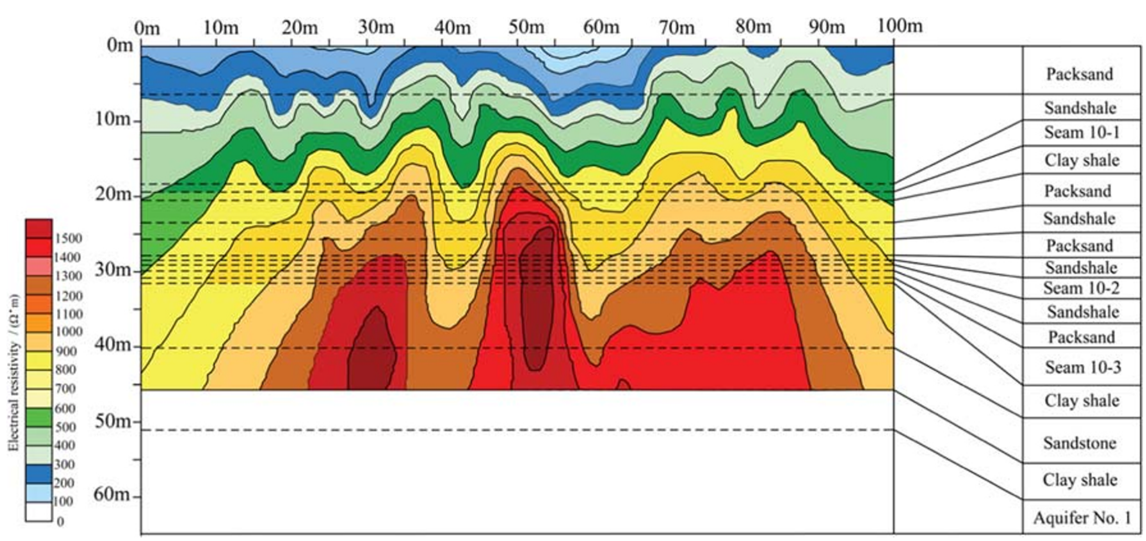

Fig. 8 Profile map of the apparent resistivity in measuring line 1 on Jun 10, 2008

the advance stress compression zone was formed in the below of coal pillars and the high resistivity zone was formed in goaf. When mining the ninth excavated coal pillars, there was an obvious characteristic of low resistivity, which had a scope of influence above − 7 m boundary, around the bottom of fine sandstone. In general, when there is the geologic body with poor electrical conductivity, the electric current will keep away from it due to current repulsion effect, which can be seen as the unbroken seam floor in dry cycle, while the geologic body with good electrical conductivity will have an attractive effect on the electric current, which can be seen as water inrush because of the plastic failure of floor strata in wet cycle (Li et al. 2015; Yang et al. 2018b). In this analysis, it was caused by the plastic failure of rock strata and then water filling, indicating that the plastic failure zone developed into a depth of 7 m.

Figure 9 shows the curve of angular displacement in borehole 1. Measuring results manifested that the angular displacement varied from different depths of rock strata. The closer the distance between coal seam and rock strata, the greater the angular displacement, meaning that the rock strata will be easier to deform and break. According to the theoretical analysis and numerical results before exploitation, the plastic failure of rock strata would occur if the angular displacement of floor sandstone is over 0.005 or 0.29°. Based on this prospected result, the angular displacement is over 0.005 or 0.29° above − 5 m boundary, indicating that the plastic failure depth of seam floor was 5 m. To sum up the above measuring results, the failure depth of seam floor in working face 9113 after strip mining was 5–7 m.

After the safe mining of working face 9113, the method of strip mining was also adopted to exploit working face 9115 but with the widths of excavated strip at 20 m and retained strip at 20 m in order to gain the influence rule of increasing width of excavated strip on seam floor's failure. Three measuring lines were also installed in working face 9115 to monitor the failure depth of seam floor. Measuring results manifested that it was feasible to properly increase the mining size in working face 9115 which was located in shallow level.

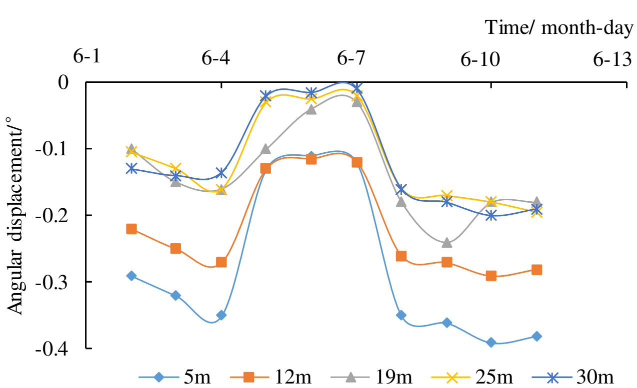

Fig. 9 Measuring curve of angular displacement in borehole 1

These physical quantities, the electrical resistivity and the angular displacement in seam floor of working face, had no abrupt change after increasing the width of excavated strip. It can be concluded from the data of parallel electrical survey system and angular displacement monitoring that the failure depth of seam floor in working face 9115 after strip mining was 5–7 m as well. However, micro-seismic monitoring results indicated that the deformation and failure of seam floor had superposition due to successive mining of working faces, making the failure depth of seam floor increase to 10 m.

Comparison with numerical results

From the numerical simulation on floor failure depth prediction, there was a plastic failure zone of 9 m in floor meaning the failure depth of seam floor. The comparison between numerical results and field measurements revealed that the simulation results are smaller than measured results. As mentioned in the simulation settings, the reason for the failure depth difference may be the neglect of coal seam dip angle (Li et al. 2018; Wu et al. 2004; Zhang 2005; Zhang and Shen 2004). In spite of this, the simulation results still had good consistency with the field measurement results, generally proving the reliability of numerical simulation. Meanwhile, as for this coal seam, according to the geological conditions and previous analysis, it showed that the main reason for the coal seam floor failure was its exploitation, while the model has fully considered the influence of such main factors, such as the excavation of coal seam and the backfilling of caving zone, on the failure depth of seam floor.

The comparison between measured data and numerical simulation results indicated the reasonability and feasibility of numerical model, meaning that the last simulation step stated in the "Influence on floor failure depth" subsection can be successfully applied to analyze the final process of proposed controlling measure for floor water inrush.

After the strip mining technology was employed in the study mining area to exploit coal resources, a mass of coal pillars were retained in order to control surface subsidence, but causing a lot of resources wasted. And can the failure depth of seam floor developed at this moment ensure the nonoccurrence of floor water inrush is still unknown.

Water inrush prevention using caving zone backfill technology

The need for excavating retained strip coal pillars, controlling surface subsidence, and preventing floor water inrush had arose further consideration. Based on previous engineering practice adopting strip mining method, the caving zone backfill technology was proposed, since the generated floor failure zone can be backfilled so that the retained coal pillars could be excavated as well as preventing floor failure. That is, the controlling measure is combined by strip mining and caving zone backfill technology to prevent the potential risk of water inrush from seam floor. Accordingly, the research of caving zone backfill technology is worthy of further attention to recover retained coal pillars in working faces. The reasonability of caving zone backfill technology and its effect on controlling surface subsidence had been stated by Zhu et al. (2018b), and the analysis in this section is mainly from the view of preventing floor water inrush to exploit coal resources above confined aquifer.

Parameter verification

To verify whether the caving zone backfill technology can be used in current mining conditions, the strength of backfilling body was initially checked by introducing the ultimate strength theory proposed in "Parameter determination" subsection. In order to guarantee the long-term stability of backfilling body, the safety factor should normally be from 1.2 to 2.0.

The corresponding meanings of some letters in Eqs. (1)–(3) have changed as follows. F is the safety factor of backfilling body, 1; σp is the strength of strip backfilling body, MPa; Pp is the load on strip backfilling body, MPa; H is the depth at which the backfilling body is located, m; We is the width of caving zone, m; Wp is the width of backfilling body, m;σm is the in situ strength of the backfilling body, MPa; and n is a constant that depends on the ratio of width to height of the backfilling body: when, $W\text{p}/h > 5$, $n = 1.4$, and when $W\text{p}/h < 5$, $n = 1$.

The maximum burial depth at which the backfilling body was located in mining area 911 was 480 m, and the height of backfilling body was 1.3 m. The UCS of the high-water content backfilling material after setting for 1 month was 2.67 MPa, and the calculated in situ strength of the backfilling body was 2.12 MPa (Zhu et al. 2018b). The strip mining working face with the widths of excavated strips at 15 m and retained strips at 20 m was subsequently recovered using caving zone backfill technology and after that the width of backfilling body was 50 m and the width of caving zone was 20 m, with a better backfilling rate of the caving zone (detailed backfilling process can be found in Zhu et al. (2018b)). Substituting these parameters into the abovementioned formulas is used to calculate the safety factor, 5.3, which was much larger than its setting range. It can be seen that the recovery scheme of excavating strip coal pillars using caving zone backfill technology in mining area 911 can ensure the long-term stability of backfilling body.

Influence on floor failure depth

On the basis of excavated numerical model in the "Floor failure depth prediction" subsection, the simulation study on exploiting retained strips using caving zone backfill technology was conducted: backfilling the caving zone after strip mining whose excavated width was 15 m and excavating retained strip coal pillars, and then backfilling the new caving zone. The replacement mining scheme with the widths of excavated strips at 20 m and retained backfilling body at 50 m was conducted to study the influence of caving zone backfill technology on failure depth of seam floor. During the backfilling period, the properties of the exploited blocks in the previous model were modified to the corresponding parameters of backfill body, which is reasonable for a high filling rate 98.7% (refer to Zhu et al. (2018b)), and then excavating the unexploited blocks between block No. 21 and No. 58 and optionally backfilling the new exploited blocks. Figure 10a shows the stress contour of surrounding rock, Fig. 10b shows the scope of plastic failure zone of floor after caving zone backfill technology, and Fig. 10c shows the distributions of the different failure values in each strip pillar respectively.

Based on the simulation results in Fig. 10, it can be shown that the plastic failure depth of seam floor had no growth (0.2 m difference probably means the effect of high-water content backfilling material, see the following) after replacement mining although the horizontal scope of plastic failure zone got larger to some extent compared with that after strip mining, and the thickness of aquiclude in seam floor had no decline when the mining scope increasing. Since the fluidity of high-water content backfilling material was perfect, mining-induced fractures in certain extent of seam floor had got backfilled after backfilling early caving zone, and then the integrity of floor had got improved as well. To sum up, the numerical results manifested that the replacement mining scheme using caving zone backfill technology in mining area 911 can prevent floor water inrush and achieve safe recovery.

Evaluation of water inrush

In terms of the prediction of floor water inrush, water inrush coefficient theory, which is based on statistical analysis of long-term inrush data and stipulated in Regulation for Coal Mine Water Prevention and Control, China (Li et al. 2018; Liu 2009; Sawsc 2009), is generally used in most of China's mining areas. The water inrush coefficient is expressed as an empirical formula:

$$T\text{s} = \frac{p}{M - CP} \tag{4}$$

where Ts is the water inrush coefficient, 1; p is the water pressure sustained by the coal seam floor, MPa; M is the thickness of aquiclude, m; and CP is the failure depth of seam floor after strip mining, m.

When the calculated water inrush coefficient is less than the critical range, the safety mining can be ensured; otherwise, floor water inrush occurs. After strip mining in mining area 911, the

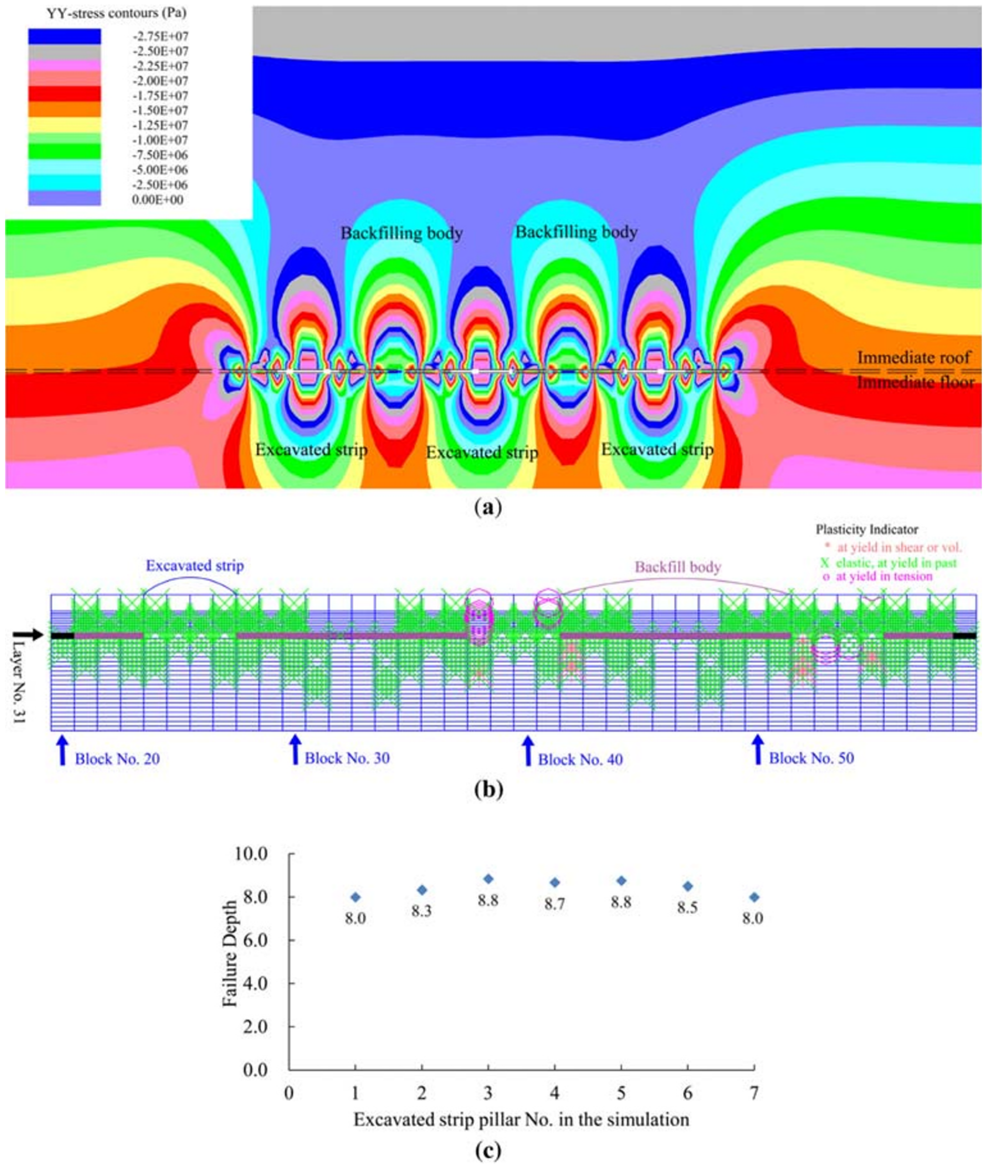

Fig. 10 Numerical results after caving zone backfill technology. **a** Vertical stress distribution contour. **b** Scope of plastic failure zone of floor. **c** Distribution of the different floor failure values in each strip pillar

failure depth of seam floor was 10 m. Therefore, the water inrush coefficient of aquifer No. 1 was $Ts1 = 4.73/(47.34 - 10) = 0.127$ Mpa/m and that of aquifer No. 2 was $Ts2 = 5.22/(84.29 - 10) = 0.070$ Mpa/m. According to the parameters in adjacent mines, the critical range of water inrush coefficient is from 0.06 to 0.10. It can be concluded that the theoretically calculated water inrush coefficients of aquifer Nos. 1 and 2 were slightly larger than the critical range after strip mining.

In view of the high-water content backfilling material used in early goaf of mining area 911, the integrity of seam floor had obtained significant improvements. The backfilling slurry flowed into failure zone of seam floor to play a reinforcing function. After the caving zone backfill technology carried out to exploit retained pillars, the width of backfilling body increased and then the bearing load on floor gained homogenized, making the failure depth of seam floor decrease under the same width of excavated strip and also decrease when successively mining working faces. The strength test for high-water content backfilling material indicated the UCS was 2.67 MPa after setting for 1 month, having an inhibiting effect on floor heave and the failure depth increase of seam floor. Besides, the strip mining practice in working face 9115 with the widths of excavated strips at 20 m and retained strips at 20 m also can demonstrate that the mining scheme with the widths of excavated strips at 20 m and retained strips at 50 m can ensure the safe recovery of working face.

Field test

The replacement mining scheme above confined aquifer using caving zone backfill technology was successively conducted in working faces 9111 and 9113, and the backfilling system, backfilling technology, and the situation of excavating the strip pillar using caving zone backfill method had been stated

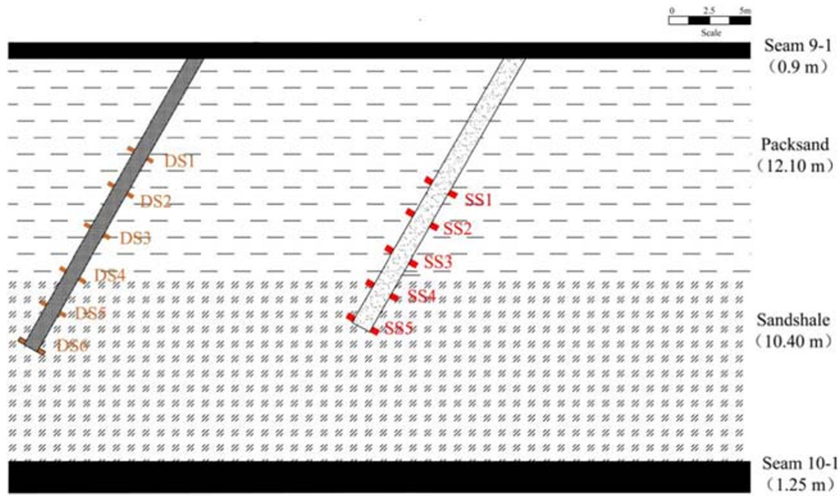

Fig. 11 Layout of the sensors in the floor (DS is the abbreviation of displacement sensor; SS is the abbreviation of stress sensor)

by Zhu et al. (2018b). In addition, in situ investigation was conducted to observe the failure depth of seam floor from the point of view of preventing floor water inrush. Prior to the backfilling and excavating, displacement and stress sensors

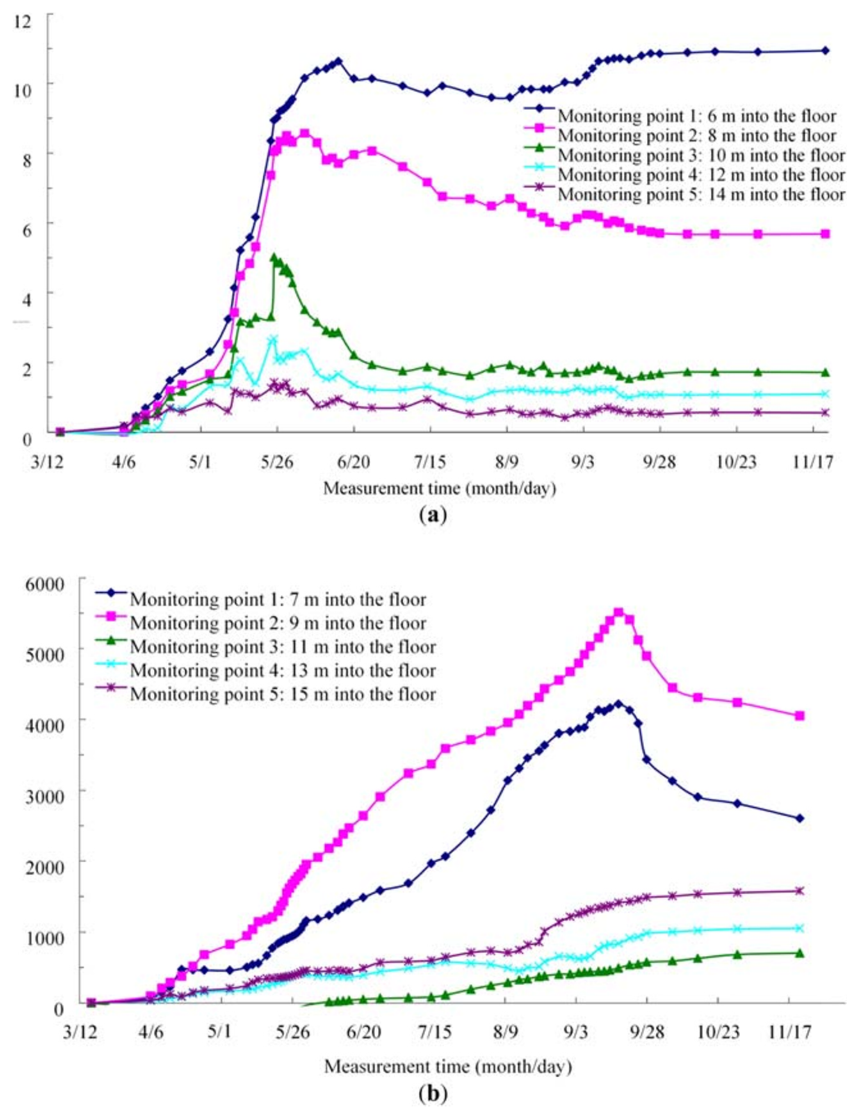

Fig. 12 Monitoring data of the sensors in the floor. **a** Displacement curves of the sensors. **b** Stain curves of the sensors (Zhu et al. 2018b)

Table 5 Displacement changes of each measuring point in the floor

Point no.	DS1	DS2	DS3	DS4	DS5	DS6
Disp/mm						
Absolute displacement	10.94	5.68	1.71	1.09	0.55	0
Relative displacement between two DSs	5.26	3.97	0.62	0.54	0.55	-

were installed in the floor of mining face 9111 to monitor changes of stress and displacement before and after mining coal seam No. 9-1. The layout of the displacement sensors and stress sensors can be seen in Fig. 11.

Six displacement monitoring points were arranged with the vertical depths being 6 m, 8 m, 10 m, 12 m, 14 m, and 16 m respectively. Fifty-three measurements were made during a period of 10 months, and the displacements of the sensors are illustrated in Fig. 12a. Five stress monitoring points were arranged with the vertical depths being 7 m, 9 m, 11 m, 13 m, and 15 m respectively. Measurements of the strains at the monitoring points are illustrated in Fig. 12b.

From absolute displacements of each monitoring point monitored by displacement sensors, relative displacements between two displacement sensors can be calculated as shown in Table 5. Thus, it can be seen that both the absolute and relative displacements of sensors 1 and 2 were large, while that of sensors 3 to 6 were small, which indicated that significant displacement occurred at 6 m and 8 m into the floor. It was also shown that the relative displacement was only 0.54–0.62 mm from 10 to 16 m into the floor. Hence, it can be concluded that the mining induced maximum depth of displacement variation in the floor was 10 m. From stress monitoring results, it can be known that the maximum micro strain occurred at the monitoring point with the vertical depth being 9 m, which indicated that the maximum failure depth was 9 m into the floor. In situ measurements of the displacement and strain indicated that when the retained pillars were excavated using caving zone backfill method, the failure depth of seam floor was still 10 m without increase. Therefore, the replacement mining practice above confined aquifer using caving zone backfill technology conducted in mining area 911 cannot only effectively prevent floor water inrush, but also achieve safe mining and recover a mass of retained coal pillars.

Further discussion

In the process of designing strip mining scheme aiming at the prevention of seam floor failure, the simulation study was only conducted on a single working face to further analyze the influence of the width of working face on floor failure, and then the maximum width of excavated strip coal pillar was obtained in overall consideration of the aquiclude thickness of floor, hydraulic pressure of aquifer No. 1, and actual situation of strip mining. Undoubtedly, this research idea needs improvement since results are mainly produced based on engineering practice and empirical evidence. The selection of strip mining scheme also had some limitations for the reason that the final determined scheme in this paper was based on the actual mining situation of several working face, which has certain dependence on practical engineering. The subsequent relevant research work can turn to the mining process or mining procedure of strip mining and on this basis, the numerical simulation study can be conducted to design the mining scheme.

As for the prediction of floor water inrush, the theoretically calculated water inrush coefficient after strip mining was slightly larger than the critical range, which indicated that there would be a great risk of floor water inrush in the study mining area if the mining scheme was not improved. The implement of caving zone backfill technology using high-water content backfill material played a recovery effect on seam floor's failure by the flow of slurry. After backfilling, although the theoretically calculated water inrush coefficient is not changed, the increased width of backfilling body made the bearing load on floor gain homogenized and the failure depth of seam floor decreases under the same width of excavated strip especially when successively mining working faces due to the compression effect of backfilling body on seam floor.

Conclusions

The core content of this paper is to decide how to exploit coal resources when there are buildings on the ground and water is abundant under the coal seam. Previous strip mining scheme can effectively control surface subsidence and achieve safe mining under buildings, but the possibility of floor water inrush was a big hidden danger and a mass of coal resources were retained in the pillars, which cannot meet the requirement of production development. However, the caving zone technology has a certain recovery effect on previous seam floor failure, and the generated backfilling body can effectively control surface subsidence and prevent water inrush from seam floor in the rest production to excavate retained coal resources. In other words, these two technologies can be linked together and bring out the best in each other. The proposed controlling measure, combined by strip mining method and caving zone backfill technology, has highlighted both advantages to prevent water inrush from seam floor and achieved safe mining above confined aquifer and under buildings to the maximum extent.

In the process of designing strip mining method, by referring to adjacent working faces which achieved safe and high-efficiency mining, the scheme of strip mining along the dip with the widths of excavated strip at 15 m and retained strip at 20 m was decided, which was also verified by numerical simulation with the failure depth of 9 m in seam floor formed. During the field trial of strip mining in the west wing of mining area 911, in situ measurements manifested that the failure depth of seam floor in working faces 9113and 9115 was 5–7 m, and micro-seismic monitoring results indicated that the failure depth of seam floor increased to 10 m due to superposition effect generated when successively advancing working faces, agreeing well with the numerical simulation result.

In the second process, a certain amount of failure depth of seam floor and the demand of exploiting retained resources in coal pillars aroused more discussion about caving zone backfill technology. The safety factor of backfilling body calculated by the ultimate strength theory indicated the long-term stability of backfilling body, and although the water inrush coefficient theory showed a potential of floor water inrush after strip mining, the caving zone backfill technology using high-water content backfilling material can make the integrity of seam floor obtain significant improvements to prevent the failure depth increasing. The simulation study on exploiting retained strips using caving zone backfill technology based on strip mining model revealed that the plastic failure depth of seam floor had no growth. Engineering practice and in situ measurements demonstrated that after excavating retained pillars by caving zone backfill technology, the failure depth of seam floor was still 10 m with no increase, which cannot only effectively prevent floor water inrush, but also achieve safe mining and recover a mass of retained coal pillars. Therefore, it can be concluded that the controlling measure, combined by strip mining method and caving zone backfill technology, is capable of bringing significant economic and environmental benefits when mining above confined aquifer and under buildings.

Acknowledgments Appreciations are given to two anonymous reviewers for their endeavor in reviewing this paper.

Funding information The financial supports from the Fundamental Research Funds for the Central Universities (2017XKQY023) are greatly appreciated.

Compliance with ethical standards

Conflict of interest The authors declare that they have no conflict of interest.

References

Bieniawski ZT (1981) Improved design of coal pillars for us mining conditions. In: Proc 1st conference on ground control in mining. Morgantown, pp 13–22

Bondarenko V, Kovalevska I, Dychkovskiy R (2010) New techniques and technologies in mining. CRC Press, London, pp 15–16

Cai W, Chang Z, Zhang D, Wang X, Cao W, Zhou Y (2019) Roof filling control technology and application to mine roadway damage in small pit goaf. Int J Min Sci Technol 29:477–482

Chatterjee R, Jain AK, Chandra S, Tomar V, Parchure PK, Ahmed S (2018) Mapping and management of aquifers suffering from over-exploitation of groundwater resources in Baswa-Bandikui watershed, Rajasthan, India. Environ Earth Sci 77:157

Dong D, Sun W, Xi S (2012) Water-inrush assessment using a GIS-based bayesian network for the 12-2 coal seam of the Kailuan Donghuantuo coal mine in China. Mine Water Environ 31:138–146

Gao W, Ge M (2016) Stability of a coal pillar for strip mining based on an elastic-plastic analysis. Int J Rock Mech Min Sci 87:23–28

Guo B, Cheng T, Wang L, Luo T, Yang X (2018) Physical simulation of water inrush through the mine floor from a confined aquifer. Mine Water Environ 37:577–585

Huang Z, Jiang Z, Zhu S, Wu X, Yang L, Guan Y (2016) Influence of structure and water pressure on the hydraulic conductivity of the rock mass around underground excavations. Eng Geol 202:74–84

Huang Z, Zeng W, Wu Y, Li S, Zhao K (2019) Experimental investigation of fracture propagation and inrush characteristics in tunnel construction. Nat Hazards 97:193–210

Junthong P, Khamrat S, Sartkaew S, Fuenkajorn K (2019) Determination of time-dependent strengths of salt pillars based on strain energy principle. Int J Min Sci Technol 29:273–279

Li L, Zhang J (1995) Calculation and prediction of water-inrush from mining floor and its application. Coal Geol Explor 23:34–38

Li S, Liu B, Nie L, Liu Z, Tian M, Wang S, Su M, Guo Q (2015) Detecting and monitoring of water inrush in tunnels and coal mines using direct current resistivity method: a review. J Rock Mech Geotech Eng 7(4):469–478

Li W, Liu Y, Qiao W, Zhao C, Yang D, Guo Q (2018) An improved vulnerability assessment model for floor water bursting from a confined aquifer based on the water inrush coefficient method. Mine Water Environ 37:196–204

Liu Q (2009) A discussion on water inrush coefficient. Coal Geol Explor 37:34–37

Ma D, Wang J, Li Z (2019) Effect of particle erosion on mining-induced water inrush hazard of karst collapse pillar. Environ Sci Pollut Res 26:19719–19728

Ma L, Du X, Wang F, Liang J (2013) Water-preserved mining technology for shallow buried coal seam in ecologically-vulnerable coal field: a

case study in the Shendong coal field of China. Disaster Adv 6:268–278
Ma L, Jin Z, Liang J, Sun H, Zhang D, Li P (2015) Simulation of water resource loss in short-distance coal seams disturbed by repeated mining. Environ Earth Sci 74:5653–5662
Malkowski P, Ulaszek A, Ostrowski L (2014) Optimization of roof coal thickness in the roof of longwall face as a result of water inflow into roof rocks. Przeglad Gorniczy Nr 3:48–57
Malkowski P, Ostrowski L, Bozecki P (2017) The impact of the mineral composition of Carboniferous claystones on the water-induced changes of their geomechanical properties. Geol Geophys Environ 43(1):43–55
Mark C, Agioutantis Z (2019) Analysis of coal pillar stability (ACPS): a new generation of pillar design software. Int J Min Sci Technol 29: 87–91
Meng Z, Li G, Xie X (2012) A geological assessment method of floor water inrush risk and its application. Eng Geol 143-144:51–60
Meng L, Feng Q, Li Q (2018) Coupled simulation–optimization model for draining confined aquifer via underground boreholes to prevent water inrush of coal mines. Environ Earth Sci 77:607
Niedbalski Z, Malkowski P, Majchercayk T (2018) Application of the NATM method in the road tunneling works in difficult geological conditions–the Carpathian flysch. Tunn Undergr Space Technol 74: 1–59
Palarski J, Plewa F, Strozik G (2011) Backfill and grouting technology in underground coal mining using saline mine water. In: Proceedings of the 10th international symposium on mining with backfill. The Southern African Institute of Mining and Metallurgy, Johannesburg, pp 15–19
Palarski J, Plewa F, Strozik G (2014) Filling of voids in coal longwall mining with caving technical-environmental and safety aspects. In: Proceedings of the 11th international symposium on mining with backfill. Australian Centre for Geomechanics, Perth, pp 483–491
Qian M, Miao X, Li L (1995) Mechanism for the fracture behaviors of main floor in longwall mining. Chin J Geotech Eng 17:55–62
Sawsc S (2009) Coal mine water prevention and control regulations. China Coal Industry Publ. House, Beijing, pp 84–85
Strozik G (2017) Reduction of saline waters discharge from coal mines through filling and sealing of underground voids. World Sci News 72:498–512
Wu Q, Wang M, Xu X (2004) Investigations of groundwater bursting into coal mine seam floors from fault zones. Int J Rock Mech Min Sci 41(4):557–571
Wu Q, Wang M (2006) Characterization of water bursting and discharge into underground mines with multilayered groundwater flow systems in the North China coal basin. Hydrogeol J 14:882–893
Wu Q, Zhou W (2008) Prediction of groundwater inrush into coal mines from aquifers underlying the coal seams in China: vulnerability index method and its construction. Environ Geol 56:245–254
Wu Q, Liu Y, Liu D, Zhou W (2011) Prediction of floor water inrush: the application of GIS-based AHP vulnerable index method to Donghuantuo coal mine, China. Rock Mech Rock Eng 44:591–600
Wu Q, Fan S, Zhou W, Liu S (2013) Application of the analytic hierarchy process to assessment of water inrush: a case study for the no. 17 coal seam in the Sanhejian coal mine, China. Mine Water Environ 32:229–238
Xu X, Wang J (1991) Prediction of coal mining water inrush. Geology Publishing House, Beijing, pp 45–48
Yang B, Yuan J, Ye Z (2018a) Risk assessment of coal mining above confined aquifer based on maximizing deviation in a GIS environment. Arab J Geosci 11:299
Yang L, Sun Q, Yang H (2018b) Laboratory-based geoelectric monitoring of water infiltration in consolidated ground. Hydrogeol J 26(7): 2229–2240
Yang T, Zhu W, Yu Q, Liu H (2011) The role of pore pressure during hydraulic fracturing and implications for groundwater outbursts in mining and tunnelling. Hydrogeol J 19:995–1008
Yin H, Wei J, Guo J, Zhu L, Shi L, Zhai P, Liu X (2009) Application of strip-partial mining to prevent water inrush from coalbed floor in Nanding coal mine. In: International Conference on Information Engineering and Computer Science, pp 1–4
Zhang L, Deng K, Zhu C, Xing Z (2011) Analysis of stability of coal pillars with multi-coal seam strip mining. Trans Nonferrous Metals Soc China 21:549–555
Zhang J (2005) Investigations of water inrushes from aquifers under coal seams. Int J Rock Mech Min Sci 42:350–360
Zhang J, Shen B (2004) Coal mining under aquifers in China: a case study. Int J Rock Mech Min Sci 41(4):629–639
Zhang S, Guo W, Li Y (2017a) Experimental simulation of water-inrush disaster from the floor of mine and its mechanism investigation. Arab J Geosci 10:503
Zhang S, Guo W, Li Y, Sun W, Yin D (2017b) Experimental simulation of fault water inrush channel evolution in a coal mine floor. Mine Water Environ 36:443–451
Zhu W, Xu J, Xu J, Chen D, Shi J (2017) Pier-column backfill mining technology for controlling surface subsidence. Int J Rock Mech Min Sci 96:58–65
Zhu W, Yu S, Xu J (2018a) Influence of the elastic dilatation of mining-induced unloading rock mass on the development of bed separation. Energies 11:785
Zhu W, Yu S, Xuan D, Shan Z, Xu J (2018b) Experimental study on excavating strip coal pillars using caving zone backfill technology. Arab J Geosci 11:554
Zingano A, Weiss A (2019) Subsidence over room and pillar retreat mining in a low coal seam. Int J Min Sci Technol 29:51–57